

We are IntechOpen, the world's leading publisher of Open Access books Built by scientists, for scientists

4,800

Open access books available

122,000

International authors and editors

135M

Downloads

Our authors are among the

154

Countries delivered to

TOP 1%

most cited scientists

12.2%

Contributors from top 500 universities



WEB OF SCIENCE™

Selection of our books indexed in the Book Citation Index
in Web of Science™ Core Collection (BKCI)

Interested in publishing with us?
Contact book.department@intechopen.com

Numbers displayed above are based on latest data collected.
For more information visit www.intechopen.com



Wavelet Correlation Analysis for Quantifying Similarities and Real-Time Estimates of Information Encoded or Decoded in Single-Trial Oscillatory Brain Waves

Takaaki Sato, Riichi Kajiwara, Ichiro Takashima and Toshio Iijima

Additional information is available at the end of the chapter

<http://dx.doi.org/10.5772/intechopen.74810>

Abstract

Even in cases when we recognize identical objects or when we behave similarly, the spatiotemporal activities in the brain are likely to fluctuate to various degrees. Temporally fluctuating responses easily decrease by averaging replicate measures. We previously developed a wavelet correlation analysis that tolerates the across-trial oscillatory phase variability observed in odor-induced cortical responses. The wavelet correlation analysis revealed a change in the neuronal information redundancy of transient and oscillatory brain waves from the dependencies on stimulus experience (high redundancy) to stimulus quality (low redundancy) between the input and output layers of the anterior piriform cortex in guinea pigs. We report on its application to estimate information in the fine temporal structures of single-trial brain waves. By using a set of standard brain waves for each information in a given category, the highest wavelet correlation coefficients provided the first candidate of estimated information with 75% accuracy. Moreover, the probability of including the correct information for the two upper candidates, regardless of information redundancy of the signal sources, was >92%. The wavelet correlation analysis is useful for similarity analyses and real-time estimates of in-brain information and for its application to brain-machine interfaces or medical/research tools.

Keywords: cross-correlation analysis, electroencephalography, information redundancy, odor representation, oscillatory local field potentials, real-time estimation, wavelet transformation

1. Introduction

In the sensory system, a stimulant likely activates stimulant-specific subsets of neurons with a stimulant-specific response profile through the sensory pathway from the sensory organ to the primary sensory cortex, resulting in identical sensory perception of the stimulant. At different stages of this neuronal information processing, the redundancy in sensory information changes by summing or subtracting overlapping signals from cognate and noncognate receptors for common and unique elements. The sensory systems generate oscillatory activities between related cortical regions and the thalamus, except in the olfactory system. The olfactory system generates oscillatory activities in the first and second olfactory centers, the olfactory bulb, and the anterior piriform cortex (aPC). It is significantly more difficult to quantify the degree of similarity or difference in these transient oscillatory responses compared to stationary oscillatory activities. We previously developed a wavelet correlation analysis that is phase-tolerant for transient oscillatory responses and demonstrated a stimulus dependency of the odor-evoked oscillatory brain waves (oscillatory local field potentials, osci-LFPs) in the aPC output layer and an experience dependency in the input layer [1]. These results suggest that the redundancy in the neural representation of olfactory information may change in the aPC.

Sensory systems are incorporated in higher brain functions that synergistically control animal behaviors through multiple neural systems including sensory, memory, decision, motor, or other systems. Generally, all neural systems would maintain the reliability of signal processing in identical activities of identical subsets of neurons in identical time courses through neural pathways with acceptable across-trial variability. This suggests that brain waves in identical behaviors could be, to some extent, reproduced in each brain. Small fluctuations, however, sometimes change oscillatory phases across trials, as has been observed in odor-induced oscillatory brain waves [1]. The fine temporal structures of phase-fluctuated oscillatory activities responsible for informational differences are easily lost by averaging several brain waves, even for identical information in each brain. Associations of single-trial brain waves with in-brain information have been rarely studied. Regarding mental states, the most important individual-independent frequencies of electroencephalography (EEG) are 7–12 Hz at the P1 electrode and <5 Hz at Fz for attention, 10–20 Hz at F4 for fatigue, and 4–7 Hz at Fz and 10–20 Hz at Cz for frustration, with even greater variations in frequencies observed across individuals [2]. Alpha-band oscillations (8–13 Hz) exert top-down influences on the early visual processing for attention orienting [3] and are sensitive markers in the auditory memory loading process [4]. As a test case, we applied a wavelet correlation analysis to estimate odor information in the fine temporal structures of single-trial brain waves.

2. Wavelet correlation analysis

2.1. Characteristics of odor-evoked oscillatory brain waves in the aPC

Odor-evoked oscillatory brain waves in the aPC are not stationary over the time window of interest, even in an *ex vivo* isolated whole brain with attached nose preparation under the

condition of no inputs from the nonolfactory sensory systems (**Figure 1**) [1, 5]. Oscillatory brain waves initiate during the 1-s odor presentation before the peak of the receptor potential, the electro-olfactogram (EOG) (the lowest trace in **Figure 1**) [1]. A pair of quite different odors, lavender essential oil (Lav), and a mixture of three fatty acids—mc4 + mc6 + mc8 (mc468)—were selected as plant- and animal-related odors, respectively. Linalool (Lina) and *n*-butanoic acid (mc4) were selected as the single-compound odors of Lav and mc468, respectively, with partial overlaps of the activated olfactory receptors and their respective signal pathways with their original mixtures as well as 0.1 Lav (10-fold diluted Lav). As expected, oscillatory brain waves of a pair of quite different Lav and mc468 odors look dissimilar in the initial phase but are partially similar in the late phase.

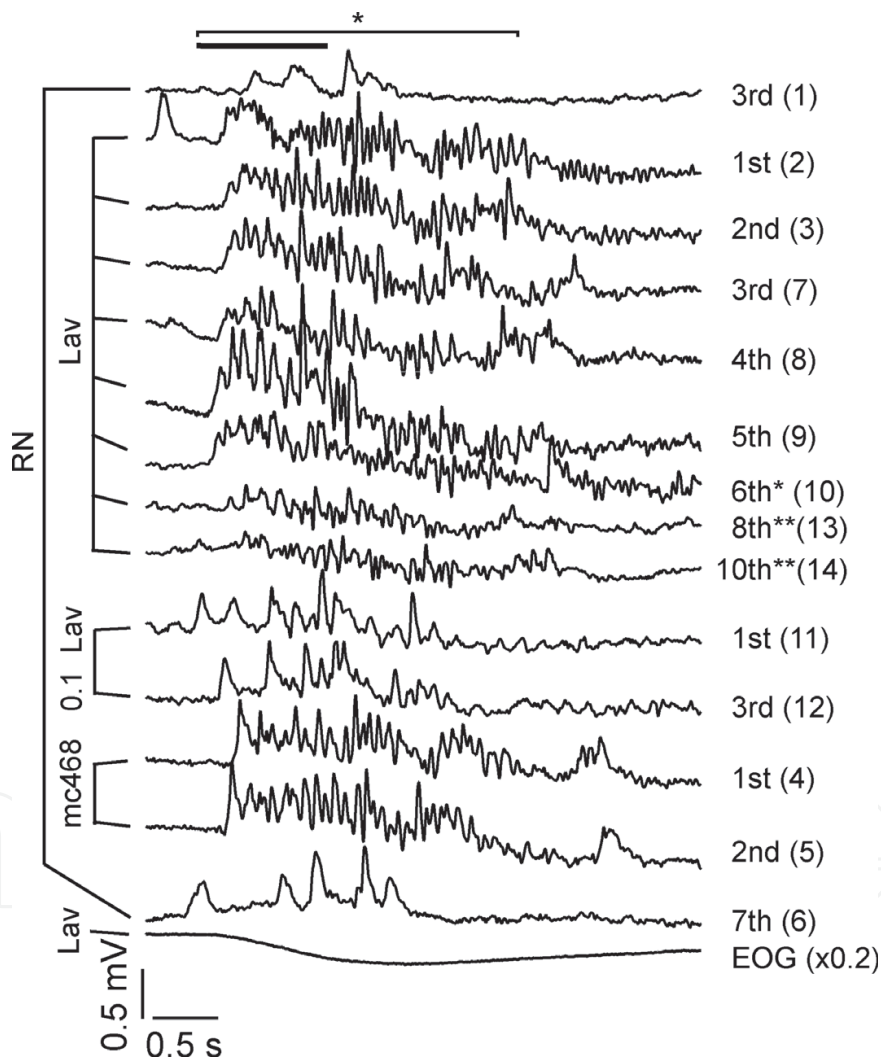


Figure 1. Odor-evoked oscillatory brain waves in layer I of the anterior piriform cortex (aPC) [1]. Time courses of low-pass-filtered (0–45 Hz) oscillatory brain waves and the receptor potential (electro-olfactogram, EOG) at the centromedial or caudocentral** site of the aPC in the isolated whole brain are shown for three odors (Lav, lavender essential oil as an odor from a plant; 0.1 Lav (10-fold diluted Lav); and mc468, a mixture of three fatty acids as an imitated odor from animals). Ringer solution (RN) was used as a control. The odor or RN was presented to the nose of the isolated brain for 1 or 4 s* (only for the sixth Lav), as indicated by the horizontal bar in the in-presentation order for each odor (entire presentation order). The responses in the 2.5-s time window* of interest were analyzed.

The correlations of the temporal profiles of oscillatory brain waves in the aPC for a 2.5-s time window, which comprised the 1-s odor presentation and the following 1.5 s, were not homogeneously high between identical odors (**Figure 2A**) [1]. Only a few identical odor pairs for Lav or 0.1 Lav demonstrated relatively high correlations (0.7–0.74), whereas the remaining pairs demonstrated intermediate (0.47–0.69) or low (0.29) correlations. These low correlations are attributable to the independent fluctuations in the oscillatory phase angles and powers including a few synchronous cycles (indicated by the daggers), in the fast Fourier transform (FFT) components even between identical odors, indicating that oscillatory responses are not strictly phase-locked to the stimulus onset (**Figure 3**) [1]. The spurious high correlations of the 0–45 Hz components are attributable to the similarities in the temporal profiles of the 0–2 Hz components [1]. The 0–2 Hz component resulted in high correlations (>0.77) for all the Lav and 0.1-Lav pairs (**Figure 2B**), whereas the 2–45 Hz components resulted in low correlations (<0.4) for all pairs (**Figure 2C**). To address these weaknesses of the conventional analyses, we tested a novel correlation analysis of wavelet profiles.

2.2. Wavelet correlation analysis procedure for oscillatory brain waves in the time window of interest

Figure 4 shows the procedure for the wavelet transformation and its conversion to a data array for the wavelet correlation analysis [1]. The wavelet time-frequency power profiles enable us to quantify the similarity of the odor-evoked oscillatory brain waves. The wavelet transform is like a running, windowed Fourier transform; it uses a certain window size and slides it along in time, computing the FFT at each time using only the data within the window. The original wavelet software libraries were provided by Torrence and Compo [6] and modified with respect to the following points. Because of the spurious high correlations in the low-frequency band, all 0–2 Hz components were removed prior to the phase-tolerant analysis of the 2–45 Hz components of the oscillatory brain waves. The 2–45 Hz bandpass-filtered brain waves (**Figure 4A**) were subjected to a Morlet wavelet analysis by using the following equations:

$$W_n(s) = \sum_{n'=0}^{N-1} x_{n'} \Psi^* \left[\frac{(n' - n)\delta t}{s} \right] \quad (1)$$

$$\Psi_0(\eta) = \pi^{-1/4} e^{i\omega_0 \eta} e^{-\eta^2/2} \quad (2)$$

$$\omega_j = \frac{\omega_0 + \sqrt{2 + \omega_0^2}}{4\pi s_j} \quad (3)$$

$$s_j = s_0 2^{j\delta j} \quad (j = 0, 1, \dots, J) \quad (4)$$

$$J = \delta j^{-1} \ln \frac{N\delta t}{s_0} \quad (5)$$

where (*) indicates the complex conjugate, $\omega_0 = 6$, $N = 2048$, $\delta t = 0.001$, $s_0 = 2\delta t$, and $\delta j = 0.1$. The wavelet power spectrum, $|W_n(s)|^2$, was plotted in the 1.89–42.78 Hz frequency (ω_j) range

A

	Lav										0.1Lav		mc468		RN
	1st	2nd	3rd	4th	5th	6th*	8th**	10th**	1st	3rd	1st	2nd	7th		
Lav	1st		0.52	0.58	0.55	0.50	0.52	0.51	0.54	-0.17	-0.19	0.15	0.31	0.09	
	2nd	0.52		0.65	0.57	0.65	0.67	0.49	0.56	-0.24	-0.16	0.21	0.40	0.23	
	3rd	0.58	0.65		0.70	0.69	0.59	0.47	0.55	-0.26	-0.15	0.27	0.44	0.16	
	4th	0.55	0.57	0.70		0.71	0.64	0.59	0.66	-0.36	-0.21	0.13	0.48	0.11	
	5th	0.50	0.65	0.69	0.71		0.73	0.62	0.62	-0.39	-0.26	0.20	0.46	0.20	
	6th*	0.52	0.67	0.59	0.64	0.73		0.55	0.56	-0.35	-0.27	0.27	0.41	0.28	
	8th**	0.51	0.49	0.47	0.59	0.62	0.55		0.64	-0.35	-0.17	0.12	0.30	0.44	
	10th**	0.54	0.56	0.55	0.66	0.62	0.56	0.64		-0.28	-0.09	0.08	0.31	0.19	
	0.1Lav	1st	-0.17	-0.24	-0.26	-0.36	-0.39	-0.35	-0.35	-0.28		0.74	-0.17	-0.45	-0.24
		3rd	-0.19	-0.16	-0.15	-0.21	-0.26	-0.27	-0.17	-0.09	0.74		-0.25	-0.34	-0.11
mc468	1st	0.15	0.21	0.27	0.13	0.20	0.27	0.12	-0.08	-0.17	-0.25		0.29	0.23	
	2nd	0.31	0.40	0.44	0.48	0.46	0.41	0.30	0.31	-0.45	-0.34	0.29		0.26	
RN	7th	0.09	0.23	0.16	0.11	0.20	0.28	0.44	0.19	-0.24	-0.11	0.23	0.26		

B

	Lav										0.1Lav		mc468		RN
	1st	2nd	3rd	4th	5th	6th*	8th**	10th**	1st	3rd	1st	2nd	7th		
Lav	1st		0.86	0.85	0.85	0.82	0.86	0.77	0.77	0.49	0.37	0.44	0.55	0.26	
	2nd	0.86		0.95	0.91	0.94	0.94	0.82	0.81	0.66	0.60	0.50	0.77	0.39	
	3rd	0.85	0.95		0.91	0.93	0.93	0.78	0.79	0.64	0.59	0.54	0.76	0.35	
	4th	0.85	0.91	0.91		0.93	0.91	0.92	0.92	0.71	0.54	0.27	0.66	0.29	
	5th	0.82	0.94	0.93	0.93		0.97	0.85	0.86	0.76	0.70	0.39	0.81	0.41	
	6th*	0.86	0.94	0.93	0.91	0.97		0.84	0.81	0.73	0.67	0.44	0.77	0.37	
	8th**	0.77	0.82	0.78	0.92	0.85	0.84		0.90	0.80	0.60	0.22	0.54	0.56	
	10th**	0.77	0.81	0.79	0.92	0.86	0.81	0.90		0.79	0.46	-0.01	0.45	0.32	
	0.1Lav	1st	0.49	0.66	0.64	0.71	0.78	0.73	0.80	0.79		0.84	0.00	0.54	0.59
		3rd	0.37	0.60	0.59	0.54	0.70	0.67	0.60	0.46	0.84		0.36	0.78	0.64
mc468	1st	0.44	0.50	0.54	0.27	0.39	0.44	0.22	-0.01	0.00	0.36		0.66	0.42	
	2nd	0.55	0.77	0.76	0.66	0.81	0.77	0.54	0.45	0.54	0.78	0.66		0.40	
RN	7th	0.26	0.39	0.35	0.29	0.41	0.37	0.56	0.32	0.59	0.64	0.42	0.40		

C

	Lav										0.1Lav		mc468	RN	
	1st	2nd	3rd	4th	5th	6th*	8th**	10th**	1st	3rd	1st	2nd	7th		
Lav	1st		-0.06	0.21	0.00	0.00	-0.11	0.06	0.08	0.05	-0.02	0.17	0.10	-0.10	
	2nd	-0.06		0.12	0.04	-0.01	0.06	-0.18	0.14	-0.02	0.04	-0.09	-0.03	0.01	
	3rd	0.21	0.12		0.27	0.16	-0.18	-0.14	0.12	0.00	0.17	0.05	0.05	-0.11	
	4th	0.00	0.04	0.27		0.11	-0.04	-0.14	0.01	0.08	0.37	0.08	0.10	-0.21	
	5th	0.00	-0.01	0.16	0.11		-0.07	0.11	-0.25	-0.13	0.11	0.17	-0.02	-0.13	
	6th*	-0.11	0.06	-0.18	-0.04	0.07		-0.20	0.04	0.25	0.02	-0.11	-0.12	0.12	
	8th**	0.06	-0.18	-0.14	-0.14	0.11	-0.20		0.00	-0.06	-0.03	0.01	0.04	0.22	
	10th**	0.08	0.14	0.12	0.01	-0.25	-0.04	0.00		-0.03	0.04	-0.18	0.09	-0.03	
	0.1Lav	1st	0.05	-0.02	0.00	0.08	-0.13	0.25	-0.06	0.03		0.20	0.01	0.08	0.14
		3rd	-0.02	0.04	0.17	0.37	0.11	0.02	-0.03	0.04	0.20		-0.19	0.13	-0.10
mc468	1st	-0.17	-0.09	-0.05	-0.08	0.17	-0.11	-0.01	-0.18	0.01	-0.19		-0.01	0.06	
	2nd	0.10	-0.03	0.05	0.10	-0.02	-0.12	0.04	0.09	0.08	0.13	-0.01		0.01	
RN	7th	-0.10	0.01	-0.11	-0.21	-0.13	0.12	0.22	-0.03	0.14	-0.10	0.06	0.01		

D

	Lav		mc468			RN				Lav		0.1Lav		Lav	
	1st	2nd	1st	2nd	7th	3rd	4th	5th	6th*	1st	3rd	8th**	10th**		
Lav	1st		0.86	0.44	0.55	0.26	0.85	0.85	0.82	0.86	0.49	0.37	0.77	0.77	
	2nd	0.86		0.50	0.77	0.39	0.95	0.91	0.94	0.94	0.66	0.60	0.82	0.81	
mc468	1st	0.44	0.50		0.66	0.42	0.54	0.27	0.39	0.44	0.00	0.36	0.22	-0.01	
	2nd	0.55	0.77	0.66		0.40	0.76	0.66	0.81	0.77	0.54	0.78	0.54	0.45	
RN	7th	0.26	0.39	0.42	0.40		0.35	0.29	0.41	0.37	0.59	0.64	0.56	0.32	
Lav	3rd	0.85	0.95	0.54	0.78	0.35		0.91	0.93	0.93	0.64	0.59	0.78	0.79	
	4th	0.85	0.91	0.27	0.66	0.29	0.91		0.93	0.91	0.71	0.54	0.92	0.92	
	5th	0.82	0.94	0.39	0.81	0.41	0.93	0.93		0.97	0.78	0.70	0.85	0.86	
	6th*	0.86	0.94	0.44	0.77	0.37	0.93	0.91	0.97		0.73	0.67	0.84	0.81	
	0.1Lav	1st	0.49	0.66	0.00	0.54	0.59	0.64	0.71	0.78	0.73		0.84	0.80	0.79
		3rd	0.37	0.60	0.36	0.78	0.64	0.59	0.54	0.70	0.67	0.84		0.60	0.46
Lav	8th**	0.77	0.82	0.22	0.54	0.56	0.78	0.92	0.85	0.84	0.80	0.60		0.90	
	10th**	0.77	0.81	-0.01	0.45	0.32	0.79	0.92	0.86	0.81	0.79	0.46	0.90		

Figure 2. Correlation matrices among odor-evoked oscillatory brain waves in layer I of the aPC [1]. (A) Matrix of cross-/autocorrelations of the 0–45 Hz components of the odor-evoked oscillatory brain waves in the 2.5-s time window* of interest (shown in Figure 1). Some of the identical odor pairs produced high correlations >0.7. Identical odors are grouped in the order of stimulus presentation. (B) Cross-/autocorrelation matrix of the 0–2 Hz components of the odor-evoked oscillatory brain waves. (C) Cross-/autocorrelation matrix of the 2–45 Hz components of the odor-evoked oscillatory brain waves. By omitting the 0–2 Hz component, all correlations were reduced to <0.4. (D) the matrix in B rearranged in the entire presentation order did not demonstrate an approach of the high correlations of the 0–2 Hz components to the diagonal line (between the dashed lines). The color represents the respective amplitude range of the cross-correlations: black, <0.60; green, 0.60–0.69; pink, 0.70–0.79; red, 0.80–0.89; orange, 0.90–0.99; and white, 1.00.

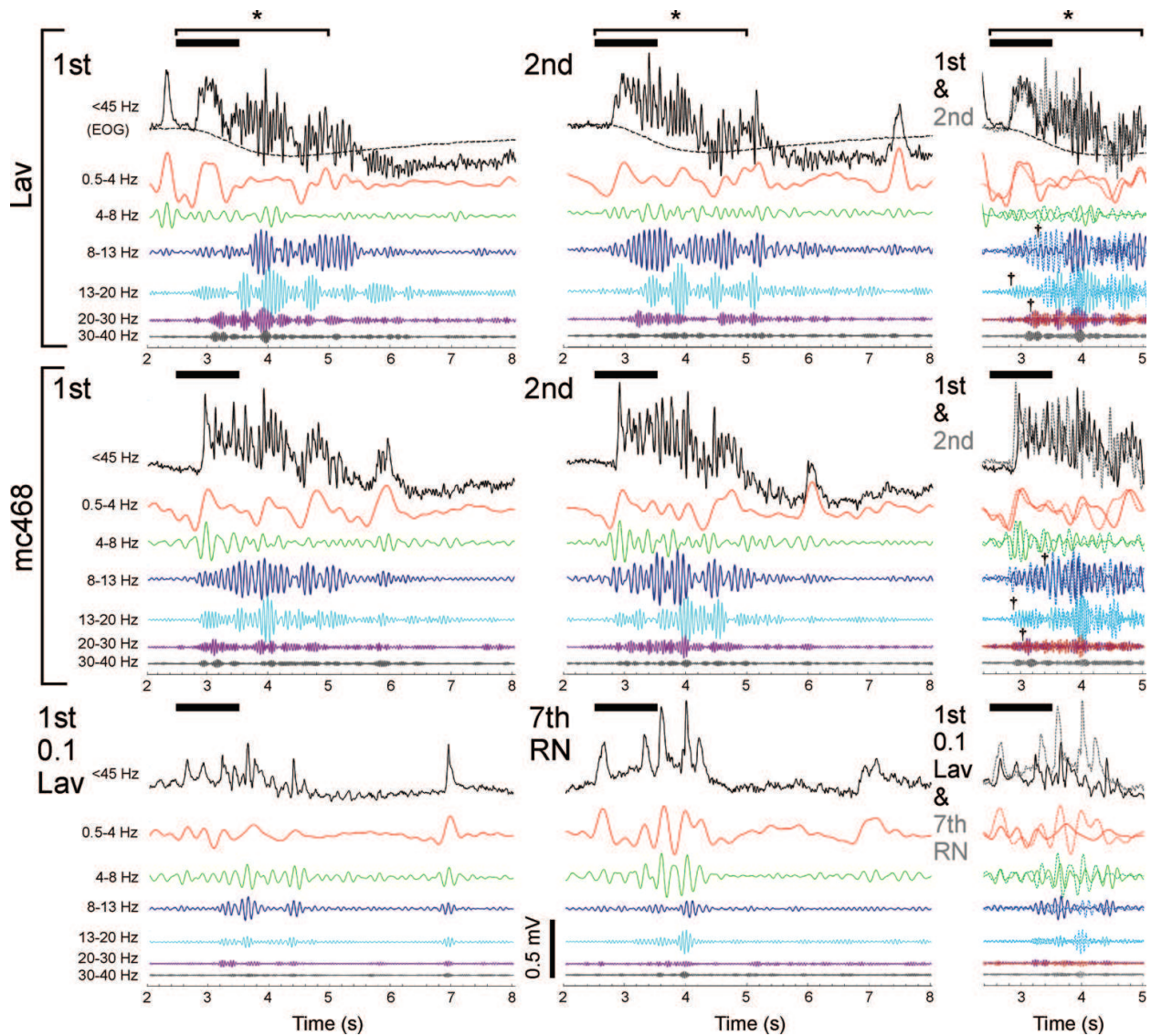


Figure 3. The oscillatory phases of the odor-evoked oscillatory brain waves differed between identical stimuli [1]. The 0–45 Hz and six frequency band components of the odor-evoked oscillatory brain waves were obtained by using an FFT bandpass filter. The two responses in the left and middle columns were superimposed on the respective frequency bands in the right column, indicating the trial-by-trial oscillatory phase differences and their fluctuations. The phase-matching points are indicated by the daggers.

(**Figure 4B**) [1]. To avoid the frequency-dependent errors that increase at the edges of epochs, the 8192 data points (2^{13} sequential points at the 1000 Hz sampling rate) were divided into seven epochs of 2048 (2^{11}) data points (2048 ms, centered every 1024 data points to the 7336th data point) with a 50% overlap and subjected to wavelet transformations (**Figure 4B**) [1]. Around the edge of each epoch, the time series was padded with the actual data ($s \geq 0$) or zeros ($s < 0$). To reconstruct a continuous wavelet transform from 0 to 8191 ms, the middle two quarters of each epoch of seven wavelets were combined (**Figure 4B**) [1]. Compared to the average wavelet power of the pre-stimulus period (10–2057 ms, marked with double asterisks in **Figure 4A**), the wavelet power in the regions within the black lines was highly significant

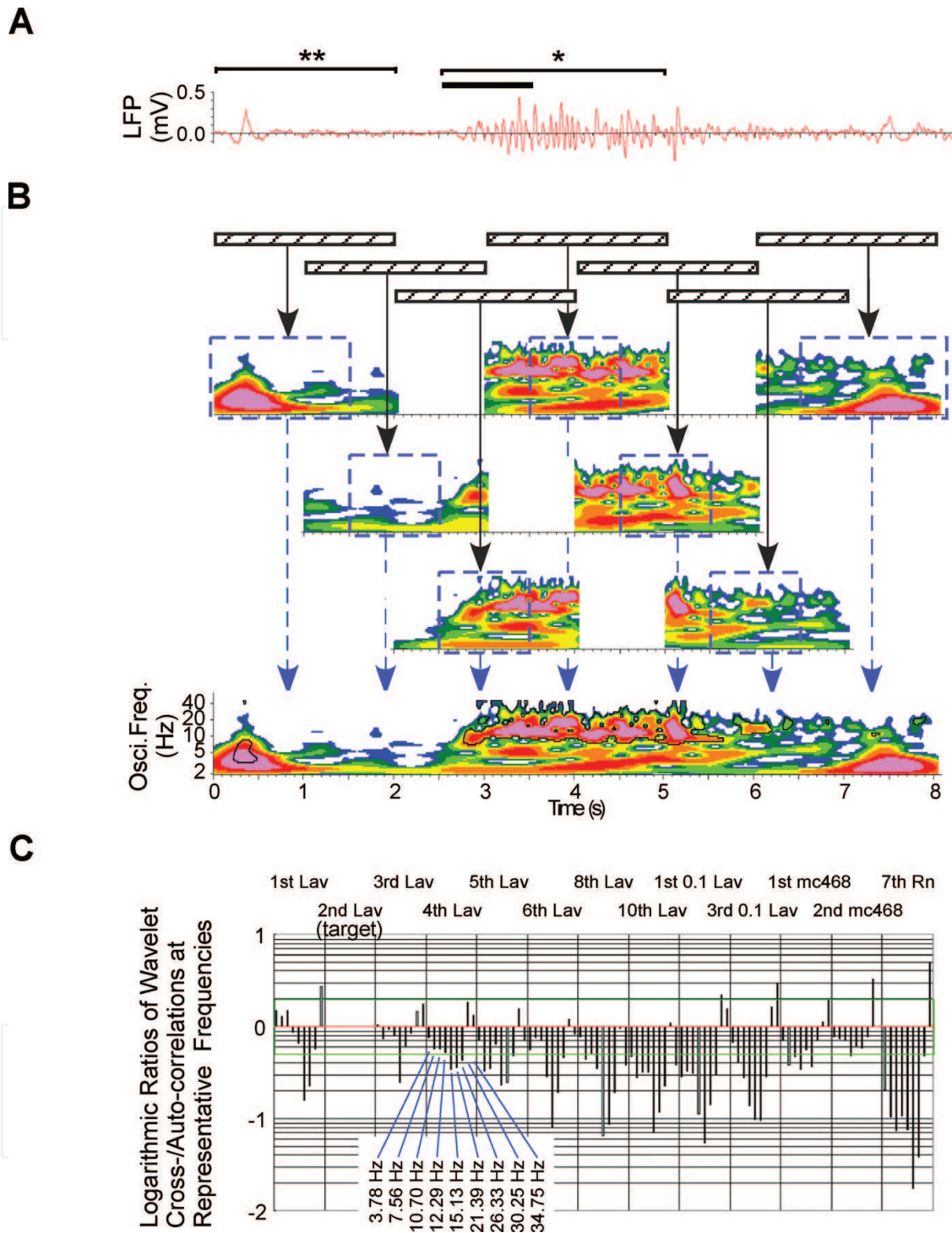


Figure 4. Wavelet transformation and wavelet cross-correlation profile of an oscillatory response [1]. (A) The 2–45 Hz component of a single-trial 1-s odor-evoked oscillatory brain wave (oscillatory local field potentials, osci-LFPs) in the anterior piriform cortex in an isolated guinea-pig whole brain (second presentation of lavender odor, indicated by the bold bar). (B) A Morlet wavelet time-frequency power spectrum of the second Lav-evoked oscillatory brain wave. Subsequently, seven sets of 2048-point wavelet transformations of the oscillatory brain waves were computed. (C) A columnar array of wavelet cross-/auto-correlations of the second Lav-evoked response. One of the responses for the 2.5-s time window at nine representative frequencies and sets of logarithmic ratios of the cross-correlation to the autocorrelation between wavelet pairs of the second Lav-evoked response (target) were serially concatenated into a data array, in which the wavelet correlations were calculated as correlation coefficients.

($P < 0.0001$, chi-squared test, **Figures 4B** and **5**) across all recordings from the same preparation at each frequency [1].

We calculated correlation coefficients between logarithmic ratio arrays of the cross-correlations to the autocorrelations of the wavelet power profile for the time window of interest at the following nine representative frequencies (selected from the calculated wavelet frequencies) to quantify the similarities of the wavelet time-frequency power profiles between identical and different odors:

Delta (2–4 Hz): 3.78 Hz.

Theta (4–8 Hz): 7.56 Hz.

Alpha (8–13 Hz): 10.7 Hz for the dominant oscillation and 12.29 Hz.

Low beta (13–20 Hz): 15.13 Hz.

High beta (20–30 Hz): 21.39 and 26.33 Hz.

Gamma (30–45 Hz): 30.25 and 34.75 Hz.

The cross-correlation was calculated as the sum of the products of the wavelet power for a pair comprising the target response ($|W_t(s, f_i)|$) and one of the other responses ($|W_n(s, f_i)|$) at the representative frequencies (f_i) for $T1 [ms] \leq s \leq T2 [ms]$. In a similar manner, the nine sums of the squared wavelet power for the target response were used to calculate the autocorrelation. Moreover, the logarithms of the ratios [$R_n(f_i)$] of the cross-correlations to the autocorrelations at the representative frequencies (f_i) were used to equalize the contributions of the increases and decreases in the response amplitude to the correlation analysis:

$$R_n(f_i) = \frac{\sum_{s=T1}^{T2} |W_n(s, f_i)| |W_t(s, f_i)|}{\sum_{s=T1}^{T2} |W_t(s, f_i)| |W_t(s, f_i)|} \quad (6)$$

A serially concatenated columnar array of all sets of the nine logarithmic ratios of the cross-correlations to the autocorrelations of the target response in the identical order of responses is a form of a wavelet cross-correlation profile (**Figure 4C**) [1]. The wavelet correlations were calculated as the correlation coefficients between these columnar arrays and employed to quantify the similarities of the odor-evoked oscillatory brain waves in the aPC.

Other mother wavelets such as Meyer and Mexican hat were considered to be inadequate for application to the odor-evoked oscillatory brain waves because their shapes appeared more dissimilar to any FFT components of the oscillatory brain waves than that of the Morlet (**Figure 3**). To date, except for one case [1], there are no published results of quantifying the similarities between oscillatory brain waves. Regarding the time-frequency power profiles, three reports were found. In one study, a discrete wavelet transform was used to identify and compare the timings of spike trains in an insect antennal lobe (corresponding to the mammal olfactory bulb) [7]. In another study, the Morlet wavelet transform was used to identify dominant oscillatory frequency bands and the synchrony between the oscillatory brain waves

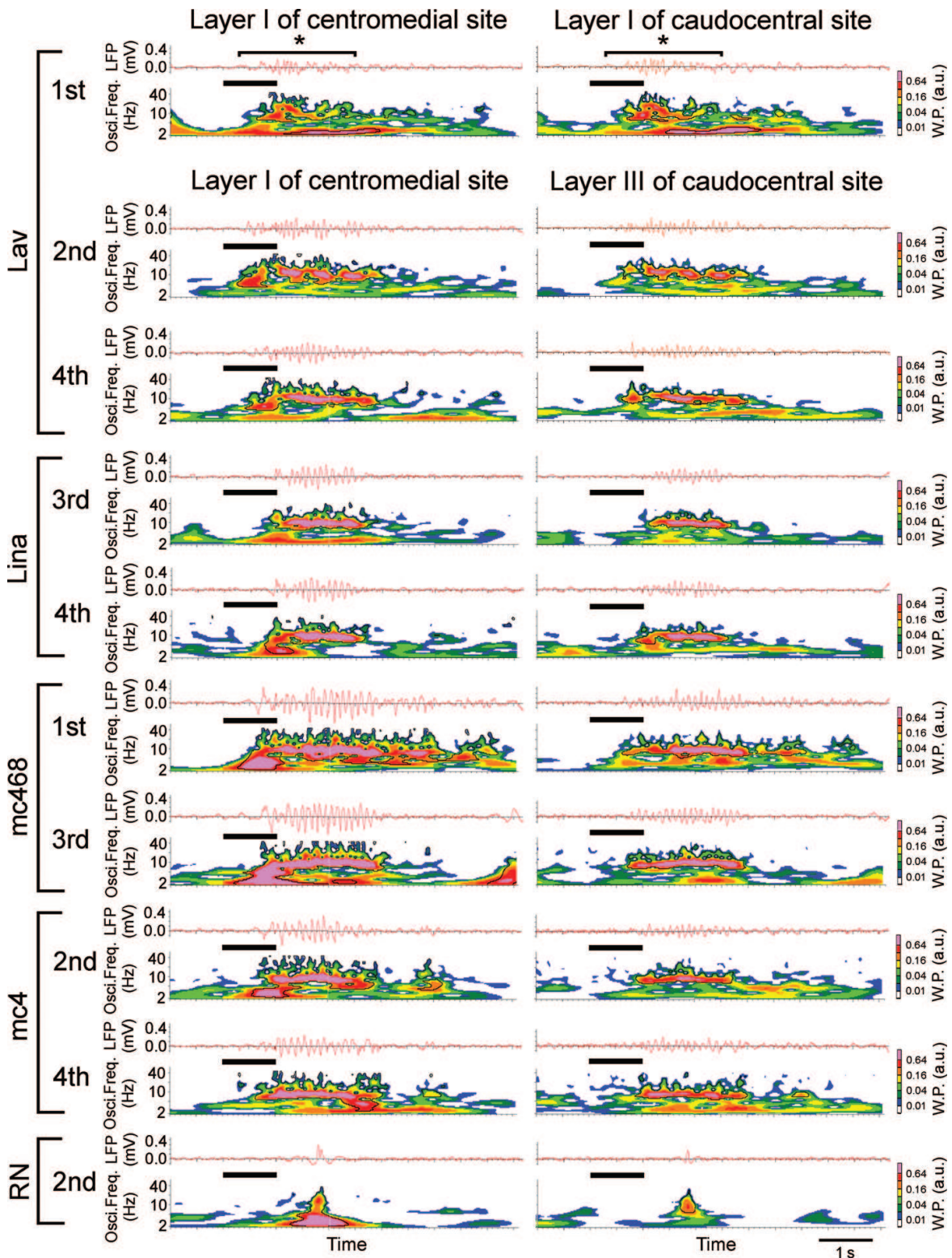


Figure 5. The wavelet profiles of odor-evoked oscillatory brain waves differed between the input and output layers of the aPC [1]. Of the 21 pairs of 1-s odor-evoked oscillatory brain waves (upper traces) that were simultaneously recorded in layers I (input) or III (output) of the aPC, 10 pairs are represented. In the wavelet time-frequency power profiles (lower traces) for the 2.2-s time window (marked by the asterisk), the ~10 Hz components remained prominent in layer III, whereas the <8 Hz components became less prominent compared to those in layer I. The in-stimulant presentation order is indicated. Statistically significant oscillatory powers were located within the black lines compared to those before presentation of odors ($P < 0.0001$, chi-squared test).

in different olfactory regions [8]. In the third study, the Hilbert transform was used to identify the dominant oscillations of the odor-evoked responses in the theta band in the posterior piriform cortex with phase-locked activities in the hippocampus in humans [9]. The Hilbert transform produced similar oscillation powers in a wide frequency range of 60–140 Hz, which is inconsistent with the decreased powers of the Morlet wavelet. Considering these results, we did not intend to analyze the odor-evoked oscillatory brain waves with the Meyer or Mexican hat mother wavelets or the Hilbert transform.

2.3. Wavelet correlation analysis of the time-frequency power profiles for revealing the stimulus dependency of odor-evoked oscillatory brain waves

The wavelet correlation analysis revealed that the olfactory information redundancy of a neural representation changes from experience (high redundancy) to a stimulus dependency (low redundancy) in the aPC [1]. The origins of the activities in layer I of the aPC are mainly the afferent fibers (input), association fibers, and postsynaptic inhibitory feedback input, whereas the activities in layer III primarily originate from the responses (output) of pyramidal cells, which are the principal neurons in the aPC and receive signals from multiple ORs. The wavelet profiles of identical odors resembled each other more than they resembled those of different odors in layers I (input signals) and III (output signals) of the aPC (**Figure 5**) [1]. In addition, the wavelet transformation visualized moderately clustered spot-like transient reductions in oscillatory power at frequencies just above 10 Hz in the odor-evoked oscillatory brain waves in layer I of the aPC (**Figure 5**). The most characteristic odor-dependent differences appeared in the initial phase of the wavelets for odor-evoked oscillatory brain waves in layer I of aPC. The mc468-evoked oscillatory brain wave was markedly greater especially at low frequencies in the initial phase than that of the Lav-evoked response [1].

The array data of the logarithmic ratios of the wavelet cross-/autocorrelations between 21 odor-evoked oscillatory brain waves differed slightly between layers I and III of the aPC (**Figure 6**) [1]. The lengths of the bars reflect the differences between a pair of oscillatory brain waves in such a way that the values of +1, 0, and -1 represent cross-correlations that are 10-fold, equal to, and one-tenth of the autocorrelation at the respective frequencies.

In layer III, the Lav odor pairs (broken yellow square in **Figure 7C**) showed homogeneously high correlations, except for the ninth Lav, whereas the identical Lav pairs in layer I resulted in more heterogeneous correlations (**Figure 7A**) [1]. In addition, the correlations between different single-component odors (Lina and mc4, in the broken blue squares in **Figure 7C**) decreased to <0.6 in layer III, whereas the corresponding correlations in layer I were mostly greater than 0.6 (**Figure 7A**) [1]. Notably, the heterogeneous correlations changed into an experience-dependent response similarity, which was observed for some of the odors in layer I of the aPC (a cluster of high correlations between the dashed lines in **Figure 7B** vs. **7A**) but was not clearly observed in layer III (**Figure 7D** vs. **7A**) as well as the 0–2 Hz components in layer I (**Figure 2D**) [1]. In layer III, the <8 Hz components decreased relative to those in layer I, with the prominent ~ 10 Hz oscillation remaining [1]. These results indicate a change in the neuronal information redundancy of transient and

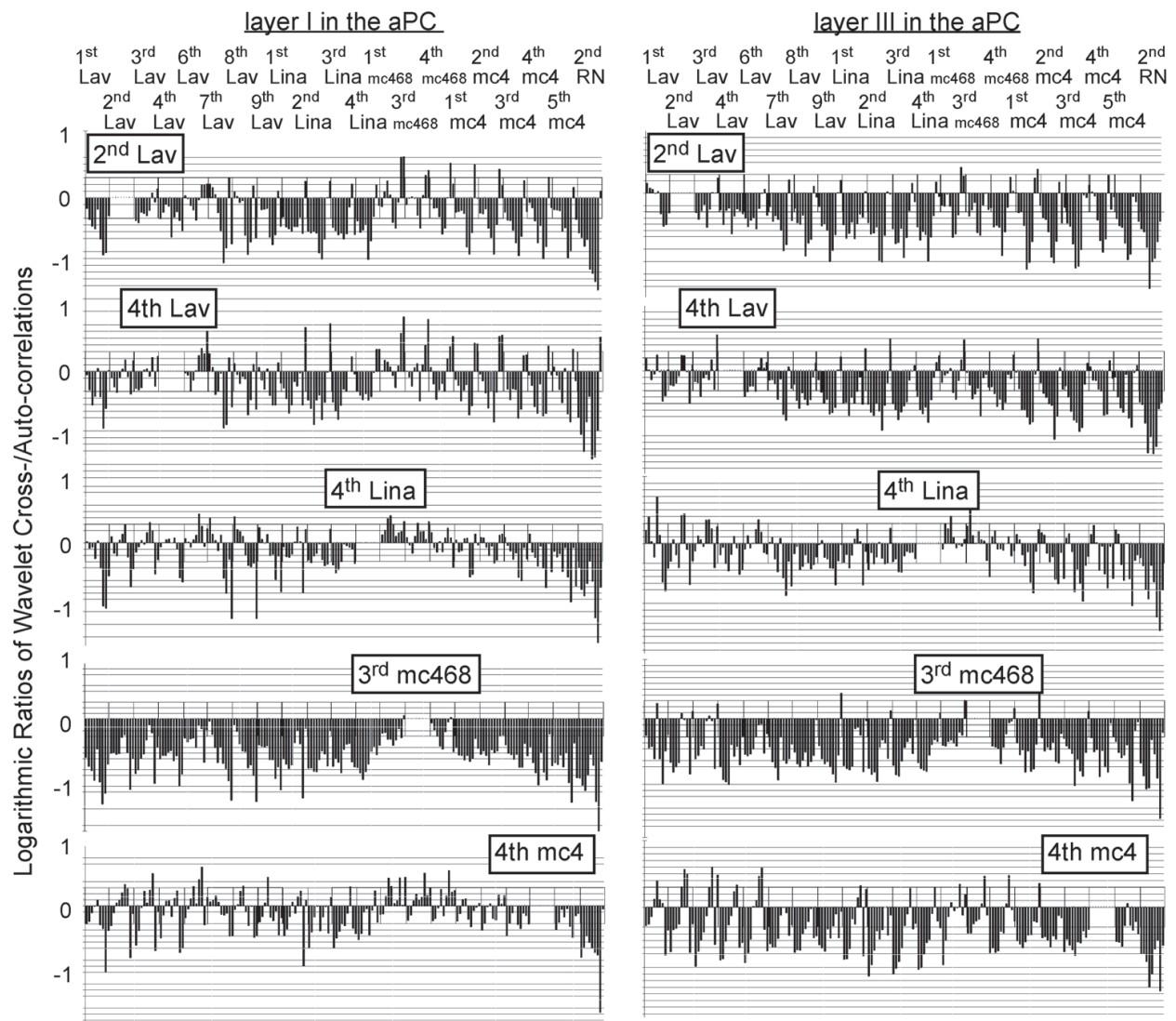


Figure 6. The wavelet cross-correlation profiles of odor-evoked oscillatory brain waves slightly differed between the input and output layers of the aPC [1]. The five pairs of logarithmic ratio arrays of the wavelet cross-/autocorrelations are exemplified. These ratio arrays suggest that the mc468-evoked responses markedly differed from those of Lav or Lina in each layer of the aPC and that they slightly differed between the input and output layers.

oscillatory brain waves from the dependencies on stimulus experience (high redundancy) to stimulus quality (low redundancy) between the input and output layers of the aPC. Recently, in the olfactory bulb that is upstream of the aPC in the olfactory pathway, stimulus history-dependent odor processing was observed [10]. This means that the wavelet correlation analysis had revealed a consistent experience dependency in input signals in the aPC from the olfactory bulb.

2.4. Effects of changes in oscillatory components on the wavelet correlation analysis

We evaluated the ability of the wavelet correlation analysis to detect changes in oscillatory powers at specific frequencies by 0.2-fold step modified wavelet powers at 1–8 frequency

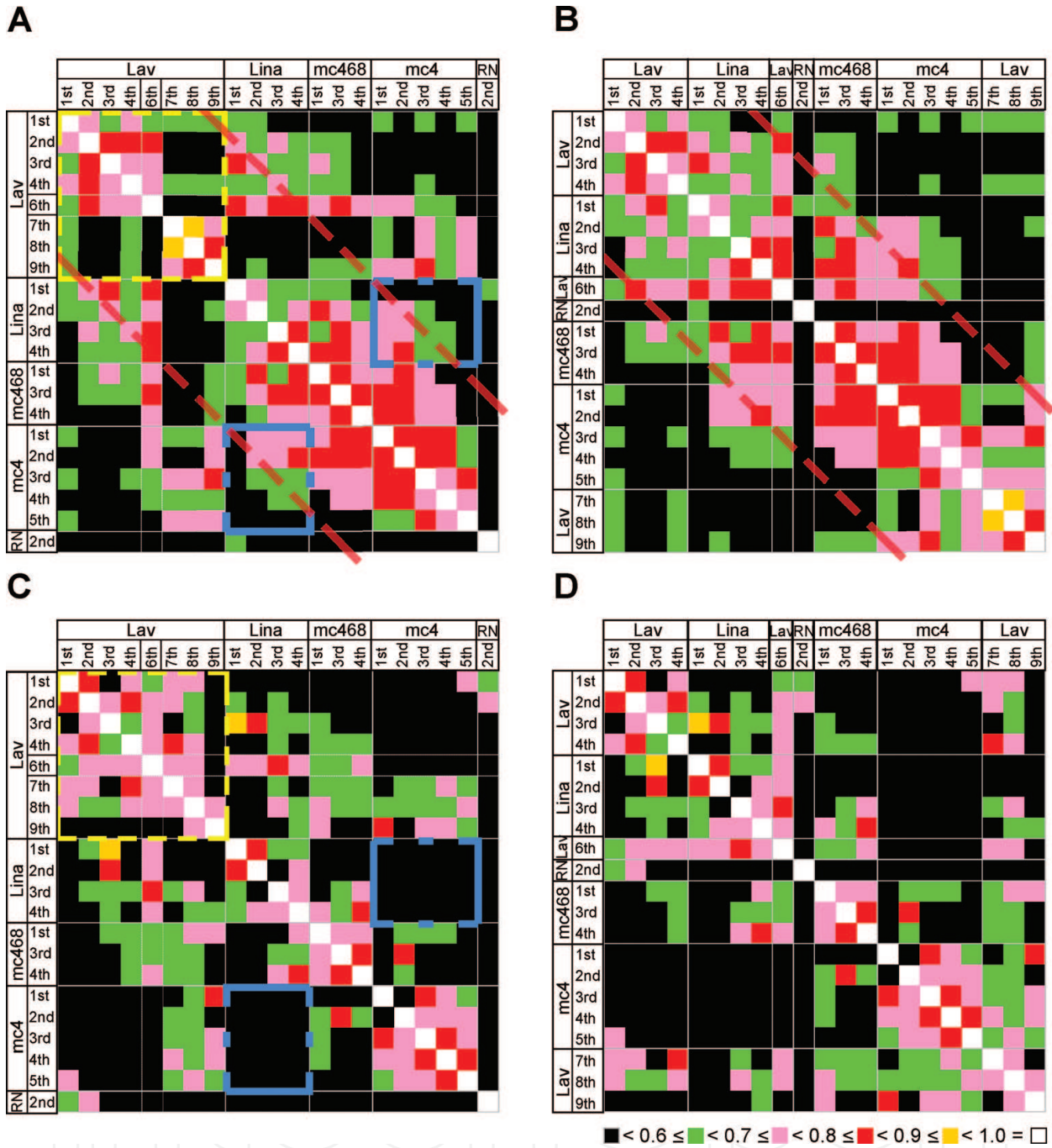


Figure 7. The wavelet correlation matrices of oscillatory brain waves differed between the input and output signals in the aPC [1]. (A) The wavelet correlation matrix of oscillatory brain waves in layer I (input) of the aPC. (B) The matrix in A rearranged in the entire presentation order. High correlations approached the diagonal line. (C) The wavelet correlation matrix of osci-LFPs in layer III (output) of the aPC. (D) The matrix in C rearranged in the entire presentation order. The colors representing power magnitudes are the same as in Figure 2.

bands (Figure 8) [1]. Greater decreases in correlations (0.4–0.7) were observed as a result of the 0.2-fold power modification at only 1–2 frequencies than those of eight frequencies (number/9 given in parentheses on the Y-axis). For 0.2-fold power amplification, the largest and smallest decreases were observed at 8–13 and 4–8 Hz, respectively. This analysis revealed that in the

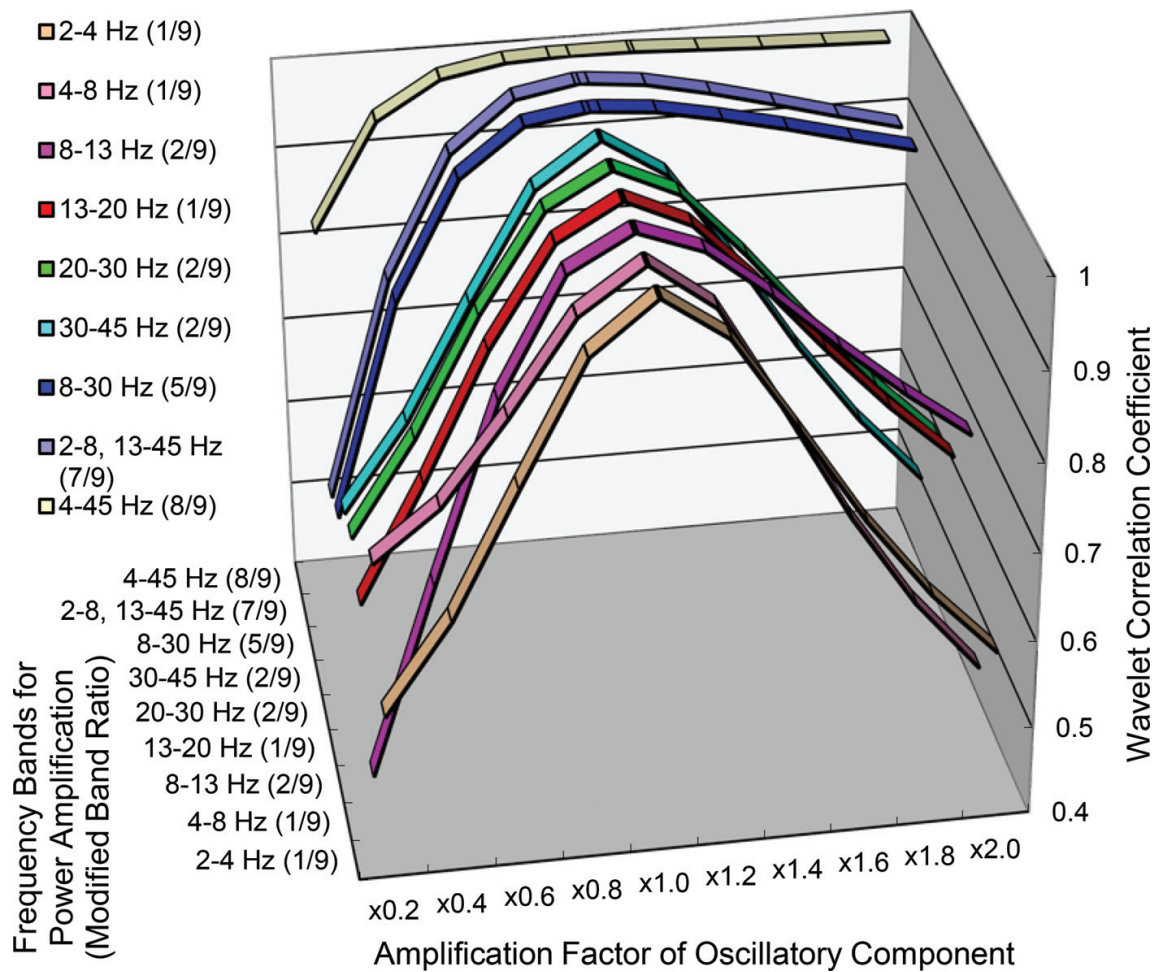


Figure 8. Sensitivity of the wavelet correlation analysis to changes in the oscillatory components [1]. A 0.2-fold power amplification resulted in the largest and smallest decreases in the wavelet correlations for 8–13 and 4–8 Hz, respectively. As the number of power-modified frequencies increased to more than four, changes in the wavelet correlations were reduced.

aPC, the 8–13 Hz component of the oscillatory brain waves contributes to the correlation coefficients more than the 4–8 Hz component. The wavelet correlation analysis enables the estimation of the relative contributions of oscillatory components to the similarities and differences between oscillatory brain waves.

3. Method for estimating in-brain information

3.1. Ranking of the correlation coefficients of several brain waves for identical information

Here, the odor-evoked brain waves were the same as those used in the previous section. To estimate the in-brain information, two standard brain waves, covering a wide range of variations for identical information, were selected. The criteria for selecting the two standard brain waves were as follows: (i) a brain wave with the highest pairwise correlation coefficient and a

high average of pairwise correlation coefficients in the given information for each individual and (ii) a brain wave with the second highest pairwise correlation coefficient and a differently ranked average of pairwise correlation coefficients in the given information for the same individual.

To select standard brain waves for the four odors, the correlation coefficients in the 2.2-s time window of interest were ranked between single-trial brain waves for all possible pairs of identical odors. Among the 28 pairs of brain waves for Lav, the highest correlation was obtained for the second Lav and fourth Lav pair that provided the fourth (median) and second highest averages of pairwise correlation coefficients, respectively (**Table 1**). The second highest correlation coefficient was obtained for the third and fifth Lav brain wave pair that provided the seventh and third highest averages of pairwise correlation coefficients, respectively. On the basis of the criteria, the fourth and third Lav brain waves were selected as the two standard brain waves for Lav information.

With regard to the pairwise correlation coefficients, their values for Lav pairs tended to be greater than those for mc4 pairs, and the values for Lina pairs tended to be greater than those for mc468 pairs. The lower correlation coefficients between identical odors suggest a greater across-trial variability in the time-frequency power profiles of single-trial brain waves, despite the tolerance of oscillatory phase differences. Similarly, the first and third Lina brain waves (**Table 2**), the fourth and first mc4 brain waves (**Table 3**), and the third and first mc468 brain waves (**Table 4**) were selected as standard brain waves for the respective information. These eight standard brain waves, as well as a control brain wave evoked by an odorless Ringer solution (second RN), were used as Set 1 of standard brain waves.

3.2. Estimates of the most probable information for single-trial brain waves using a pair of standard brain waves for each item of information

Using the wavelet correlation analysis, all possible pairwise correlation coefficients between a given single-trial brain wave and each standard brain wave (Set 1) were calculated. The first candidate was selected as the standard brain wave with the highest correlation coefficient to a target single-trial brain wave. The wavelet correlation analysis provided the first candidates for 12 single-trial brain waves with an accuracy of 75% (**Table 5**). An accuracy of 100% was achieved for Lina (2/2) and mc468 (1/1), whereas an accuracy of 67% was achieved for Lav (4/6) and mc4 (2/3). Notably, the single-trial brain waves tested were not any of the Set 1 standard brain waves. The accuracy of the first candidates was more than threefold higher than chance in five cases (20%). The probability of including the correct information for the two upper candidates was 92% (**Table 5**). However, the third candidates did not improve the probability of including the correct information for the three upper candidates (92%). In the estimates of information, candidates with correlation coefficients <0.6 were disregarded as nonspecific ones.

To compare the ideal set of standard brain waves (Set 1) with different sets of standard brain waves (standard Set 1-m) in terms of their accuracies for estimating information, wavelet correlation analyses were performed with partial replacements of standard brain waves. When one or three of the nine Set 1 standard brain waves were replaced with brain waves that did

Lav	Ranking of wavelet correlations									Standard set												
	First Lav	Second Lav	Third Lav	Fourth Lav	Sixth Lav	Seventh Lav	Eighth Lav	Ninth Lav	Corr. coeff. Rank	Ave. corr. Coeff.	Ave. rank	Memo.	1	1-m1	1-m1p1	1-mp	2	2-m2p	s1	s1 m1	s2	
First Lav	1.00	0.63995	0.26	0.59	0.44	0.59	0.60	0.31	6	0.55	6											
Second Lav	0.64	1.00	0.60	0.73	0.60	0.52	0.47	0.11	1	0.59	4	median					○	○				
Third Lav	0.26	0.60	1.00	0.47	0.683	0.28	0.54	0.38	2	0.53	7	△	○	○	○							○
Fourth Lav	0.59	0.73	0.47	1.00	0.68	0.64	0.50	0.21	1	0.60	2	⊙	○	○	○	○	○	○	○	○		
Sixth Lav	0.44	0.60	0.683	0.682	1.00	0.55	0.51	0.30	2	0.60	3											
Seventh Lav	0.59	0.52	0.28	0.63998	0.55	1.00	0.59	0.41	5	0.57	5											
Eighth Lav	0.60	0.47	0.54	0.50	0.51	0.59	1.00	0.66	4	0.61	1				○							
Ninth Lav	0.31	0.11	0.38	0.21	0.30	0.41	0.66	1.00	4	0.42	8											

Table 1. Pairwise wavelet correlations of single-trial brain waves for Lav in layer III of the aPC, their ranking, and various sets of standard brain waves.

Lina	Ranking of wavelet correlations								Standard set								
	First Lina	Second Lina	Third Lina	Fourth Lina	Corr. coeff. Rank	Ave. corr. Coeff.	Ave. rank	Memo.	1	1- m1	1- m1p1	1- mp	2	2- m2p	s1	s1 m1	s2
First Lina	1.00	0.49	0.22	0.04	1	0.44	1	⊙	○	○		○	○		○		
Second Lina	0.49	1.00	-0.13	0.18	1	0.38	3	Median			○	○	○	○			
Third Lina	0.22	-0.13	1.00	0.34	2	0.36	4	△	○								
fourth Lina	0.04	0.18	0.34	1.00	2	0.39	2			○	○		○		○		○

Table 2. Pairwise wavelet correlations of single-trial brain waves for Lina in layer III of the aPC, their ranking, and various sets of standard brain waves.

mc4	Ranking of wavelet correlations								Standard set									
	First mc4	Second mc4	Third mc4	Fourth mc4	Fifth mc4	Corr. coeff. Rank	Ave. corr. Coeff.	Ave. rank	Memo.	1	1- m1	1- m1p1	1- mp	2	2- m2p	s1	s1 m1	s2
First mc4	1.00	0.04	0.467	0.35	0.15	2	0.40	5	△	○	○			○				
Second mc4	0.04	1.00	0.25	0.366	0.368	4	0.40	4										
Third mc4	0.467	0.25	1.00	0.46	0.18	2	0.47	2					○					
Fourth mc4	0.35	0.37	0.46	1.00	0.472	1	0.53	1	⊙	○	○	○	○	○	○	○	○	○
Fifth mc4	0.15	0.37	0.18	0.472	1.00	1	0.43	3	Median	○			○					

Table 3. Pairwise wavelet correlations of single-trial brain waves for mc4 in layer III of the aPC, their ranking, and various sets of standard brain waves.

mc468	Ranking of wavelet correlations					Standard set										
	First mc468	Third mc468	Fourth mc468	Corr. coeff. Rank	Ave. corr. Coeff.	Ave. rank	Memo.	1	1- m1	1- m1p1	1- mp	2	2- m2p	s1	s1 m1	s2
First mc468	1.00	0.14	0.05	2	0.39	3	△	○	○							
Third mc468	0.14	1.00	0.23	1	0.46	1	⊙	○	○	○	○	○	○	○	○	○
Fourth mc468	0.05	0.23	1.00	1	0.43	2	Median		○	○	○	○				

Table 4. Pairwise wavelet correlations of single-trial brain waves for mc468 in layer III of the aPC and various sets of standard brain waves.

Standard brain waves	Third Lav	Fourth Lav	First Lina	Third Lina	First mc468	Third mc468	First mc4	Fourth mc4	Second RN	Highest corr.			
Third Lav	1.00	0.67	0.85	0.66	0.63	0.50	0.44	0.36	0.45	Lina			
Fourth Lav	0.67	1.00	0.58	0.61	0.70	0.54	0.28	0.54	0.41	mc468			
First Lina	0.85	0.58	1.00	0.60	0.58	0.40	0.41	0.30	0.46	Lav			
Third Lina	0.66	0.61	0.60	1.00	0.63	0.72	0.54	0.58	0.41	mc468			
First mc468	0.63	0.70	0.58	0.63	1.00	0.728	0.63	0.723	0.40	mc468			
Third mc468	0.50	0.54	0.40	0.72	0.73	1.00	0.50	0.63	0.52	mc468			
First mc4	0.44	0.28	0.41	0.54	0.63	0.50	1.00	0.73	0.35	mc4			
Fourth mc4	0.36	0.54	0.30	0.58	0.72	0.63	0.73	1.00	0.37	mc4			
Second RN	0.45	0.41	0.46	0.41	0.40	0.52	0.35	0.37	1.00	—			
Single-trial brain waves										Estimated information	Second candidate (>0.6)	Third candidate (>0.6)	
First Lav	0.56	0.77	0.47	0.48	0.53	0.47	0.39	0.59	0.49	Lav	—	—	
Second Lav	0.69	0.82	0.62	0.56	0.51	0.43	0.26	0.41	0.58	Lav	Lav	—	
Sixth Lav	0.774	0.78	0.766	0.79	0.69	0.51	0.40	0.46	0.39	Lina	Lav	Lav	
Seventh Lav	0.53	0.79	0.42	0.65	0.71	0.63	0.50	0.75	0.51	Lav	mc4	mc468	
Eighth Lav	0.641	0.693	0.52	0.689	0.68	0.56	0.63	0.63	0.33	Lav	Lina	mc468	
Ninth Lav	0.51	0.43	0.46	0.61	0.73	0.51	0.74	0.72	0.20	mc4	mc468	mc4	
Second Lina	0.71	0.44	0.79	0.53	0.56	0.29	0.48	0.29	0.28	Lina	Lav	—	
Fourth Lina	0.652	0.56	0.654	0.79	0.71	0.63	0.57	0.47	0.24	Lina	mc468	Lina	
Fourth mc468	0.58	0.56	0.54	0.775	0.777	0.86	0.60	0.63	0.33	mc468	mc468	Lina	
Second mc4	0.36	0.44	0.23	0.60	0.68	0.84	0.58	0.80	0.51	mc468	mc4	mc468	
Third mc4	0.35	0.35	0.25	0.55	0.66	0.61	0.81	0.85	0.34	mc4	mc4	mc468	
Fifth mc4	0.36	0.45	0.25	0.57	0.54	0.55	0.68	0.81	0.41	mc4	mc4	—	
										Correct rate	75%	92%	92%

Table 5. Estimated information of single-trial brain waves in layer III of the aPC by ranking of wavelet correlations using two standard brain waves (set 1).

not meet the criteria, there were no changes in the 75% accuracy for the first candidates, and a 92% probability of including the correct information for the two upper candidates was observed. Nevertheless, there were some exchanges between correct and incorrect estimates for identical information (data not shown).

In contrast, by using the pair of brain waves with the highest pairwise correlation coefficients as the two standard brain waves for each odor (standard Set 2), the accuracies of estimation were reduced by 100% for Lina ($2/2 \rightarrow 0/2$) and 34% for Lav ($4/6 \rightarrow 2/6$), but no change occurred for mc468 ($1/1$) and mc4 ($2/3$) (Table 6). This standard Set 2 provided a total accuracy of 42% (33% reduction) and a 75% probability (17% reduction) of including the correct information for the two upper candidates (Figure 9). By replacing two of the nine Set 2 standard brain waves with one that did not meet the criteria, the accuracy for the first candidates increased by 25% and the 92% probability of including the correct information for the two upper candidates was recovered (Figure 9). Therefore, the proposed criteria of selecting standard brain waves with a wide variation are likely appropriate and achieve better estimation than the selection of those with a narrow range (the most similar brain wave pairs).

3.3. Estimates of the most probable information for single-trial brain waves with a standard brain wave for each item of information

By using a set of single standard brain waves for four odors that met only the first criterion (standard Set s1), a similar accuracy of estimated information and probability of including the correct information for the two upper candidates was obtained for the 12 target brain waves (data not shown). The Set s1 standard brain waves were composed of the fourth Lav, first Lina, third mc468, fourth mc4, and second RN. Among the 16 target brain waves, the accuracy and probability slightly decreased by 6 and 4%, respectively, compared to those of the 12 target brain waves (data not shown). When one or two of the five Set-s1 standard brain waves were replaced with those that did not meet the criteria, the accuracy was reduced to 67 or 42%, respectively (data not shown). The probability of including the correct information for the two upper candidates was also reduced by 9 and 25%, respectively. For the 16 target brain waves, the accuracy and probability showed almost no changes when one of the five Set s1 standard brain waves was replaced, whereas the accuracy and probability for the estimated information were reduced by 13% when two of the Set s1 standard brain waves were replaced (data not shown).

3.4. Single-trial brain waves composed of redundant signals in the olfactory pathway exhibiting a similar accuracy and probability for estimated information

It is interesting to examine the accuracy of the wavelet correlation analysis for predicting the in-brain information of single-trial brain waves comprising redundant signals in layer I of the aPC. By using a set of standard brain waves that meet the proposed criteria for the redundant brain waves recorded in layer I (standard Set 1r), the wavelet correlation analysis provided a similar accuracy (75%) of estimated information and probability (100%) of including the correct information for the two upper candidates (Table 7) compared to the results observed for the brain waves recorded in layer III (Table 5). In contrast, by using the pairs of brain waves

Standard brain waves	Second Lav	Fourth Lav	First Lina	Second Lina	Third mc468	Fourth mc468	Fourth mc4	Fifth mc4	Second RN	Highest corr.		
Second Lav	1.00	0.80	0.57	0.47	0.40	0.37	0.35	0.39	0.55	Lav		
Fourth Lav	0.80	1.00	0.47	0.37	0.50	0.54	0.50	0.46	0.35	Lav		
First Lina	0.57	0.47	1.00	0.80	0.38	0.56	0.28	0.24	0.42	Lina		
Second Lina	0.47	0.37	0.80	1.00	0.28	0.49	0.29	0.29	0.27	Lina		
Third mc468	0.40	0.50	0.38	0.28	1.00	0.85	0.54	0.55	0.48	mc468		
Fourth mc468	0.37	0.54	0.56	0.49	0.85	1.00	0.58	0.53	0.29	mc468		
Fourth mc4	0.35	0.50	0.28	0.29	0.54	0.58	1.00	0.83	0.27	mc4		
Fifth mc4	0.39	0.46	0.24	0.29	0.55	0.53	0.83	1.00	0.38	mc4		
Second RN	0.55	0.35	0.42	0.27	0.48	0.29	0.27	0.38	1.00	—		
Single-trial brain waves												
										Estimated information	Second candidate (>0.6)	Third candidate (>0.6)
First Lav	0.78	0.76	0.42	0.36	0.44	0.41	0.58	0.70	0.43	Lav	Lav	mc4
Third Lav	0.61	0.58	0.87	0.76	0.49	0.62	0.35	0.36	0.41	Lina	Lina	mc468
Sixth Lav	0.65	0.73	0.70	0.74	0.56	0.71	0.41	0.52	0.32	Lina	Lav	mc468
Seventh Lav	0.62	0.74	0.36	0.40	0.57	0.63	0.72	0.65	0.41	Lav	mc4	mc4
Eighth Lav	0.61	0.68	0.47	0.52	0.57	0.63	0.65	0.72	0.33	mc4	Lav	mc4
Ninth Lav	0.27	0.40	0.42	0.42	0.47	0.60	0.75	0.70	0.18	mc4	mc4	mc468
Third Lina	0.52	0.57	0.55	0.54	0.69	0.77	0.54	0.60	0.40	mc468	mc468	mc4
Fourth Lina	0.34	0.50	0.62	0.70	0.60	0.84	0.44	0.40	0.18	mc468	Lina	Lina
First mc468	0.50	0.66	0.56	0.55	0.71	0.79	0.66	0.55	0.35	mc468	mc468	mc4
First mc4	0.17	0.22	0.37	0.45	0.45	0.57	0.75	0.68	0.27	mc4	mc4	—
Second mc4	0.26	0.42	0.21	0.15	0.83	0.70	0.71	0.72	0.48	mc468	mc4	mc4
Third mc4	0.19	0.32	0.24	0.28	0.60	0.63	0.85	0.77	0.28	mc4	mc4	mc468
Correct rate										42%	75%	75%

Table 6. Estimated information of single-trial brain waves in layer III of the aPC by ranking of wavelet correlations using two standard brain waves with the highest pairwise correlation coefficients (set 2).

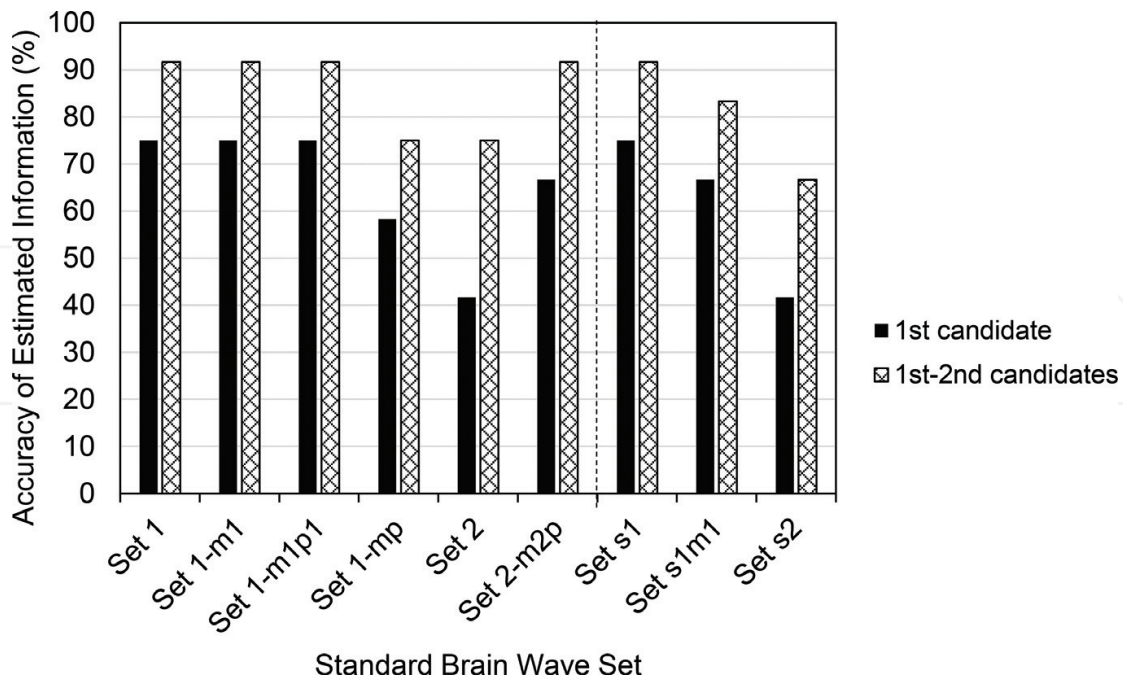


Figure 9. Variation-dependent changes in the accuracy of estimated information of single-trial brain waves in layer III of the aPC.

corresponding to the Set 1 of layer III (standard Set 1' in layer I), the accuracy of estimation was reduced by 17%, and the probability of including the correct information for the two upper candidates was reduced by 25% (to 75%) (data not shown). By using single standard brain waves (standard Set s1r), the accuracy and probability were slightly reduced compared to those of the standard Set s1 (data not shown).

Finally, it was examined whether the combination of data for two recording sites (layers I and III) affected the accuracy for the first candidates. Using this method, the accuracy (75%) of estimated information was maintained but not improved in standard Set 1 + 1' and Set 1r + 1r' (data not shown).

3.5. A new method of real-time estimation of in-brain information of single-trial brain waves

A new method is proposed for estimating the information of single-trial brain waves in fine temporal structures with a cross-trial variability by using a set of standard brain waves in a given category for each individual. In the oscillatory brain waves recorded in layer III or I of the aPC of the isolated whole brain of a guinea pig, the wavelet correlation analysis provided a 75% accuracy for the first candidate and a > 92% probability of including the correct information for the two upper candidates (Tables 5 and 7). The results support the validity of the proposed criteria for selecting standard brain waves with a wide variation for estimating different information in a given category.

The accuracy of this method was not affected by the information redundancy of signal sources, such as those resulting from olfactory receptors with overlapping tuning specificities and an

Standard brain waves	Second Lav	Eighth Lav	Second Lina	Third Lina	First mc468	Fourth mc468	First mc4	Fifth mc4	Second RN	Highest corr.			
Second Lav	1.00	0.56	0.64	0.73	0.63	0.56	0.59	0.42	0.47	Lina			
Eighth Lav	0.56	1.00	0.47	0.50	0.57	0.63	0.66	0.76	0.09	mc4			
Second Lina	0.64	0.47	1.00	0.67	0.85	0.68	0.76	0.49	0.48	mc468			
Third Lina	0.73	0.50	0.67	1.00	0.69	0.75	0.74	0.48	0.25	mc468			
First mc468	0.63	0.57	0.85	0.69	1.00	0.79	0.81	0.54	0.35	Lav			
Fourth mc468	0.56	0.63	0.68	0.75	0.79	1.00	0.87	0.58	0.23	mc4			
First mc4	0.59	0.66	0.76	0.74	0.81	0.87	1.00	0.69	0.30	mc468			
Fifth mc4	0.42	0.76	0.49	0.48	0.54	0.58	0.69	1.00	0.20	Lav			
Second RN	0.47	0.09	0.48	0.25	0.35	0.23	0.30	0.20	1.00	—			
Single-trial brain waves										Estimated information			
										Second candidate (>0.6)	Third candidate (>0.6)		
First Lav	0.77	0.70	0.66	0.52	0.59	0.55	0.63	0.70	0.43	Lav	mc4		
Third Lav	0.79	0.43	0.74	0.60	0.72	0.49	0.51	0.38	0.48	Lav	mc468		
Fourth Lav	0.83	0.68	0.58	0.70	0.66	0.58	0.61	0.53	0.20	Lav	Lav		
Sixth Lav	0.81	0.52	0.79	0.85	0.78	0.73	0.75	0.52	0.37	Lina	mc468		
Seventh Lav	0.56	0.91	0.45	0.47	0.53	0.59	0.64	0.76	0.06	Lav	mc4		
Ninth Lav	0.56	0.83	0.62	0.48	0.68	0.67	0.72	0.76	0.28	Lav	mc468		
First Lina	0.73	0.44	0.78	0.66	0.69	0.55	0.54	0.38	0.63	Lina	mc468		
Fourth Lina	0.59	0.40	0.7758	0.84	0.85	0.75	0.7756	0.42	0.27	mc468	Lina		
Third mc468	0.64	0.55	0.77	0.837	0.83	0.89	0.839	0.51	0.36	mc468	Lina		
Second mc4	0.52	0.62	0.69	0.77	0.84	0.891	0.887	0.64	0.27	mc468	mc468		
Third mc4	0.53	0.779	0.71	0.64	0.775	0.778	0.84	0.80	0.18	mc4	Lav		
Fourth mc4	0.59	0.65	0.57	0.67	0.65	0.79	0.85	0.70	0.21	mc4	mc4		
										Correct rate	75%	100%	100%

Table 7. Estimated information of single-trial brain waves in layer I of the aPC by ranking of wavelet correlations using two standard brain waves (set 1r).

Information	Recoding sites	Estimated information			
		Lav	Lina	mc468	mc4
Lav	Layer I (input)	62.8%	20.9% (e)	9.3% (e)	7.0% (e)
	Layer III (output)	57.9%	18.4% (e)	1.3% (e)	22.4% (e)
Lina	Layer I (input)	0.0% (e)	53.3%	46.7% (e)	0.0% (e)
	Layer III (output)	7.7% (e)	73.1%	19.2% (e)	0.0% (e)
mc468	Layer I (input)	0.0% (e)	25.0% (e)	75.0%	0.0% (e)
	Layer III (output)	0.0% (e)	26.7% (e)	73.3%	0.0% (e)
mc4	Layer I (input)	4.5% (e)	0.0% (e)	13.6% (e)	81.8%
	Layer III (output)	0.0% (e)	0.0% (e)	30.8% (e)	69.2%

Table 8. Correct and error rates (e) of estimated information in single-trial brain waves recorded in layers I and III of the aPC by the wavelet correlation analysis.

experience dependency in layer I or from pyramidal cells with a stimulus dependency after the integration of signals from multiple cognate olfactory receptors in layer III (**Table 8**). Layer I brain waves comprising redundant signals exhibited a similar accuracy of estimated information and a slightly increased probability of including the correct information for the two upper candidates compared to layer III brain waves.

The redundancies of brain waves are attributable to two origins: information and signaling. In the olfactory system, the information redundancy changes through the signal pathway from the receptors to the higher cortical areas via signal integration in the third- or higher-order neurons and/or mutual inhibition [1, 11–13] for category [14] or elemental odor representation [15]. Unlike the >80% overlap of about 70 receptors for carvone enantiomers having similar odors [16], the quite different odors of Lav and mc468 evoked different amplitude receptor potentials in the olfactory epithelium and dissimilar brain waves in the anterior piriform cortex [1]. Nevertheless, the wavelet correlation analysis sometimes produced the highest correlation coefficients of Lav for mc468. The error rate of Lav for mc468 was 9.3% in layer I brain waves but was reduced to 1.7% in layer III brain waves (**Table 8** and **Figure 10**), which is consistent with the change in the information redundancy from high to low stages between layers I and III. On the other hand, the error rate of mc468 for Lav was 0% in both layers I and III. For the single-compound odors, Lina and mc4 exhibited odor similarity-dependent changes in the error rates of the estimated information between layers I and III. The error rates of the single compounds for their original mixture odors (partially similar odor) increased between layers I and III (0 → 7.7% in Lina and 13.6 → 30.8% in mc4) and those of single compounds for their nonrelative mixture odors (dissimilar odor) decreased between layers I and III (46.7 → 19.2% in Lina and 4.5 → 0% in mc4). Notably, the error rates between these single compounds were 0% in both layers I and III. These results suggest a partial overlap of the elemental odors that are represented in the pyramidal cells in the aPC and are recorded in layer III as brain waves. The total error rates of Lina decreased in layer III compared to those of layer I (and vice versa for the correct rate), whereas those of mc4 increased.

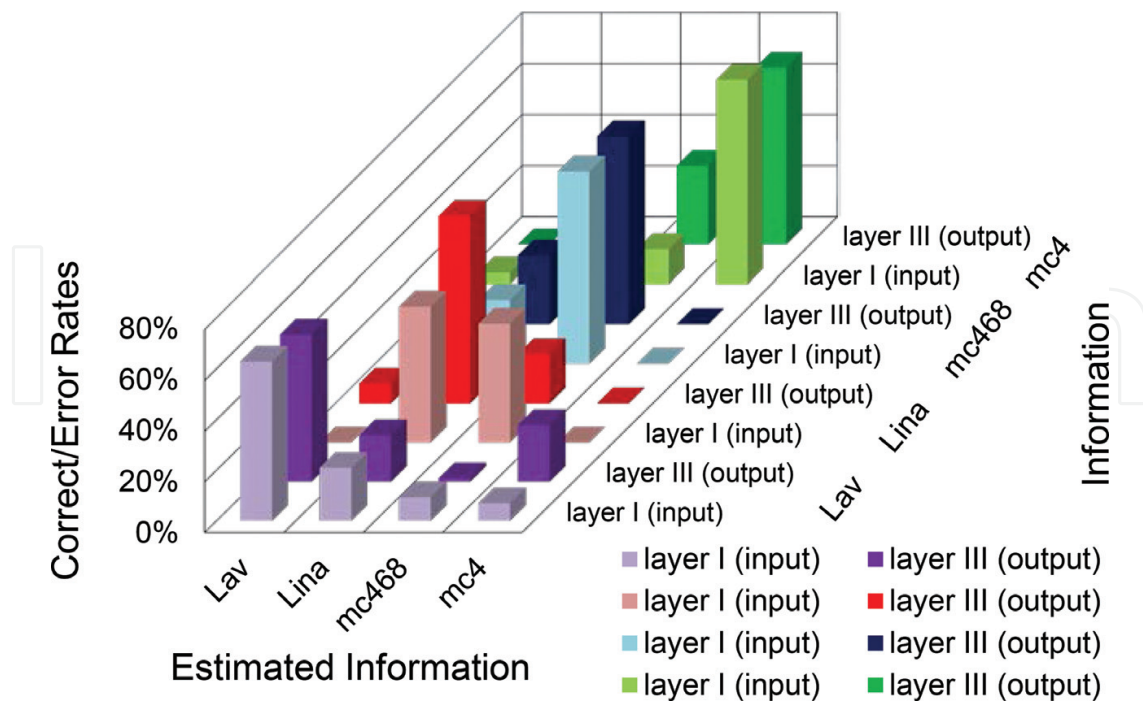


Figure 10. Correct and error rates of estimated information in single-trial brain waves recorded in layers I and III of the aPC by the wavelet correlation analysis. These values are listed in **Table 8**.

The signaling redundancy originates from an identical temporal profile of different subsets of neurons tuned to distinct or shared information or from identical temporal profiles that are composed of multiple different profiles of various different subsets of neurons tuned to multiple distinct or shared information. The constant error rates of mc468 for Lina between layers I and III (both ~25%, **Table 8** and **Figure 10**) are likely attributable to the signaling redundancy rather than the information similarity or information redundancy. Moreover, in the increased case, there was a threefold higher error rate of Lav for mc4 in layer III than layer I, whereas the error rates of Lav for Lina were almost constant between layers I and III.

3.6. Applicable examples of estimated in-brain information in humans using the wavelet correlation analysis

Each brain system (e.g., a sensory, memory, decision, or motor system) is organized in a hierarchical manner from simple to complicated matters. The sensory system generates oscillatory activities between the related cortical regions and the thalamus, and the latter acts (except in the olfactory system) to gate the sensory input to the cortex and provides feedback from the cortical pyramidal neurons. In olfaction, transient oscillatory brain waves are observed in the aPC [5, 17–21]. Strong feed-forward inhibition [5, 22, 23] via the sensitive pathway from the olfactory bulb [24] and the other sensory thalamocortical circuit [25, 26] or higher olfactory centers [27] could induce oscillatory brain waves that would contribute to parts of the EEGs recorded at the respective positions on the human scalp, in analogy to these experimental animals. Such information-dependent temporal profiles of the EEGs may enable us to estimate in-brain information by comparison with a set of standard time-frequency

power profiles of EEGs in each individual. To this aim, a wavelet correlation analysis of the brain waves in a guinea pig was conducted using standard brain waves with the proposed criteria and achieved an accuracy of 75% for the first candidates. This accuracy is attributable to the comparisons with standard single-trial responses in the wavelet time-frequency power profiles.

Conventional methods have focused only on some parts of the brain wave characteristics. For example, the FFT power spectra of sensorimotor EEGs [28, 29] or auditory EEGs [30] in specific frequency bands at a specific recording position were analyzed for the development of brain-computer interfaces. The Morlet wavelet convolutions for four-frequency band powers of the single-trial EEGs were analyzed to understand the cognitive control system via a priori estimation of information across three tasks [31]. By using the wavelet correlation analysis in the time-frequency power profiles at nine frequencies, these analyses could be improved in their subprocesses. Odor sensation [32, 33] and color-opponent responses [34] were also recorded in humans at Fz and an intermediate position between Oz and the inion, respectively, and they demonstrated informational differences in response amplitudes or profiles. Like EEGs in object recognition and those responsible for mental states, these EEGs are also subjects for the application of the wavelet correlation analysis for estimating in-brain fine information. Pain-related alpha-band desynchronization at contralateral-central electrodes (C2, C4, CP2, and CP4) and gamma-band synchronization at the ipsilateral-posterior electrodes (P3, P5, and so on) [35] are also good candidates for application. In animal models, the neural pathways of innate and learned fear responses have been revealed [36], and different pathways of stress relaxation using rose and hinokitiol odors were found [37, 38]. Therefore, determining their differing time-frequency power profiles would enable us to estimate the strengths of stress or relaxation in EEGs in humans. Future studies will focus on programming the wavelet correlation analysis for real-time estimates of in-brain information in humans.

4. Conclusions

We developed a new method for a similarity analysis and real-time estimates of in-brain information in single-trial brain waves by ranking the correlation coefficients in the wavelet correlation analysis. The wavelet correlation analysis with a set of standard brain waves provided the first candidate of estimated information with an accuracy of 75% with a > 92% probability of including the correct information for the two upper candidates, regardless of the information redundancy of signal sources. This method may be also useful for its applications to brain-machine interfaces or medical/research tools.

Acknowledgements

We would like to thank Dr. Mutsumi Matsukawa for his contributions to the development of the isolated whole-brain experimental system that enabled the recordings of odor-induced and

nonolfactory origin-free brain waves. We are also grateful to Kiyo Murano for writing the computer software for wavelet transformation. This work was supported by grants (T.S.) from METI, Japan, and Grant-in-Aids for Scientific Research (B) #15H02730 (T.S.) from the MEXT, Japan.

Abbreviations

aPC	anterior piriform cortex
aPCvr	ventro-rostral region of the aPC
EEG	electroencephalography
EOG	electro-olfactogram
FFT	fast Fourier transform
LFP	local field potential
LOT	lateral olfactory tract
OR	olfactory receptor
osci-LFP	oscillatory local field potential

Author details

Takaaki Sato^{1*}, Riichi Kajiwara², Ichiro Takashima³ and Toshio Iijima⁴

*Address all correspondence to: taka-sato@aist.go.jp

1 Biomedical Research Institute, National Institute of Advanced Industrial Science and Technology (AIST), Ikeda, Japan

2 School of Science and Technology, Meiji University, Kawasaki, Japan

3 Human Technology Research Institute, AIST, Tsukuba, Japan

4 Graduate School of Life Sciences, Tohoku University, Sendai, Japan

References

- [1] Sato T, Kajiwara R, Takashima I, Iijima T. A novel method for quantifying similarities between oscillatory neural responses in wavelet time-frequency power profiles. *Brain Research*. 2016;**1636**:107-117. DOI: 10.1016/j.brainres.2016.01.054
- [2] Myrden A, Chau T. A passive EEG-BCI for single-trial detection of changes in mental state. *IEEE Transactions on Neural Systems and Rehabilitation Engineering*. 2017;**25**:345-356

- [3] Doesburg SM, Bedo N, Ward LM. Top-down alpha oscillatory network interactions during visuospatial attention orienting. *NeuroImage*. 2016;**132**:512-519. DOI: 10.1016/j.neuroimage.2016.02.076
- [4] Wilsch A, Obleser J. What works in auditory working memory? A neural oscillations perspective. *Brain Research*. 2016;**1640**:193-207. DOI: 10.1016/j.brainres.2015.10.054
- [5] Ishikawa T, Sato T, Shimizu A, de Curtis M, Kakei T, Iijima T. Odour-driven activity in the olfactory cortex of an in vitro isolated guinea-pig whole brain with olfactory epithelium. *Journal of Neurophysiology*. 2007;**97**:670-679
- [6] Torrence C, Compo GP. A practical guide to wavelet analysis. *Bulletin of the American Meteorological Society*. 1998;**79**(61-78)
- [7] Capurro A, Baroni F, Kuebler LS, Kárpáti Z, Dekker T, Lei H, Hansson BS, Pearce TC, Olsson SB. Temporal features of spike trains in the moth antennal lobe revealed by a comparative time-frequency analysis. *PLoS One*. 2014;**9**:e84037. DOI: 10.1371/journal.pone.0084037
- [8] Pardo-Bellver C, Martínez-Bellver S, Martínez-García F, Lanuza E, Teruel-Martí V. Synchronized activity in the main and accessory olfactory bulbs and vomeronasal amygdala elicited by chemical signals in freely behaving mice. *Scientific Reports*. 2017;**7**:9924. DOI: 10.1038/s41598-017-10089-4
- [9] Jiang H, Schuele S, Rosenow J, Zelano C, Parvizi J, Tao JX, Wu S, Gottfried JA. Theta oscillations rapidly convey odor-specific content in human piriform cortex. *Neuron*. 2017;**94**:207-219
- [10] Vinograd A, Livneh Y, Mizrahi A. History-dependent odor processing in the mouse olfactory bulb. *The Journal of Neuroscience*. 2017;**37**:12018-12030
- [11] Desmaisons D, Vincent JD, Lledo P-M. Control of action potential timing by intrinsic subthreshold oscillations in olfactory bulb output neurons. *The Journal of Neuroscience*. 1999;**19**:10727-10737
- [12] Kashiwadani H, Sasaki YF, Uchida N, Mori K. Synchronized oscillatory discharges of mitral/tufted cells with different molecular receptive ranges in the rabbit olfactory bulb. *Journal of Neurophysiology*. 1999;**82**:1786-1792
- [13] Stettler DD, Axel R. Representations of odor in the piriform cortex. *Neuron*. 2009;**63**:854-864. DOI: 10.1016/j.neuron.2009.09.005
- [14] Yoshida I, Mori K. Odorant category profile selectivity of olfactory cortex. *The Journal of Neuroscience*. 2007;**27**:9105-9114
- [15] Sato T, Kawasaki T, Mine S, Matsumura H. Functional role of the C-terminal amphipathic helix 8 of olfactory receptors and other G protein-coupled receptors. *International Journal of Molecular Sciences*. 2016;**17**(pii):E1930. DOI: 10.3390/ijms17111930
- [16] Hamana H, Hirono J, Kizumi M, Sato T. Sensitivity-dependent hierarchical receptor codes for odours. *Chemical Senses*. 2003;**28**:87-104

- [17] Bressler SL, Freeman WG. Frequency analysis of olfactory system EEG cat, rabbit, and rat. *Electroencephalography and Clinical Neurophysiology*. 1980;**50**:19-24
- [18] Ketchum KL, Haberly LB. Synaptic events that generate fast oscillations in piriform cortex. *The Journal of Neuroscience*. 1993;**13**:3980-3985
- [19] de Curtis, M, Biella, G, Forti, M, Panzica, F. Multifocal spontaneous epileptic activity induced by restricted bicuculline ejection in the piriform cortex of the isolated guinea pig brain. *Journal of Neurophysiology* 1994;**71**:2463–2476
- [20] Chapman CA, Xu Y, Haykin S, Racine RJ. Beta-frequency (15-35 Hz) electroencephalogram activities elicited by toluene and electrical stimulation in the behaving rat. *Neuroscience*. 1998;**86**:1307-1319
- [21] Chabaud P, Ravel N, Wilson DA, Mouly AM, Vigouroux M, Farget V, Gervais R. Exposure to behaviourally relevant odour reveals differential characteristics in rat central olfactory pathways as studied through oscillatory activities. *Chemical Senses*. 2000;**25**:561-573
- [22] Sato T, Hirono J, Hamana H, Ishikawa T, Shimizu A, Takashima I, Kajiwara R, Iijima T. Architecture of odour information processing in the olfactory system. *Anatomical Science International*. 2008;**83**:195-206. DOI: 10.1111/j.1447-073X.2007.00215.x
- [23] Sato T, Kobayakawa R, Kobayakawa K, Emura M, Itohara S, Kizumi M, Hamana H, Tsuboi A, Hirono J. Supersensitive detection and discrimination of enantiomers by dorsal olfactory receptors: Evidence for hierarchical odour coding. *Scientific Reports*. 2015;**5**: 14073. DOI: 10.1038/srep14073
- [24] Igarashi KM, Ieki N, An M, Yamaguchi Y, Nagayama S, Kobayakawa K, Kobayakawa R, Tanifuji M, Sakano H, Chen WR, Mori K. Parallel mitral and tufted cell pathways route distinct odor information to different targets in the olfactory cortex. *The Journal of Neuroscience*. 2012;**32**:7970-7985. DOI: 10.1523/JNEUROSCI.0154-12.2012
- [25] Bruno RM. Synchrony in sensation. *Current Opinion in Neurobiology*. 2011;**21**:701-708. DOI: 10.1016/j.conb.2011.06.003
- [26] Kajiwara R, Tominaga T, Takashima I. Olfactory information converges in the amygdaloid cortex via the piriform and entorhinal cortices: Observations in the guinea pig isolated whole-brain preparation. *The European Journal of Neuroscience*. 2007;**25**:3648-3658. DOI: 10.1111/j.1460-9568.2007.05610.x
- [27] Schoenbaum G, Eichenbaum H. Information coding in the rodent prefrontal cortex. I. Single-neuron activity in orbitofrontal cortex compared with that in pyriform cortex. *Journal of Neurophysiology*. 1995;**74**:733-750
- [28] Cincotti F, Mattia D, Aloise F, Bufalari S, Astolfi L, De Vico Fallani F, Tocci A, Bianchi L, Marciani MG, Gao S, Millan J, Babiloni F. High-resolution EEG techniques for brain-computer interface applications. *Journal of Neuroscience Methods*. 2008;**167**:31-42
- [29] Cincotti F, Mattia D, Aloise F, Bufalari S, Schalk G, Oriolo G, Cherubini A, Marciani MG, Babiloni F. Non-invasive brain-computer interface system: Towards its application as assistive technology. *Brain Research Bulletin*. 2008;**75**:796-803. DOI: 10.1016/j.brainresbull.2008.01.007

- [30] Nijboer F, Furdea A, Gunst I, Mellinger J, McFarland DJ, Birbaumer N, Kübler A. An auditory brain-computer interface (BCI). *Journal of Neuroscience Methods*. 2008;**167**:43-50
- [31] Cooper PS, Darriba Á, Karayanidis F, Barceló F. Contextually sensitive power changes across multiple frequency bands underpin cognitive control. *NeuroImage*. 2016;**132**:499-511. DOI: 10.1016/j.neuroimage.2016.03.010
- [32] Tonoike M. Emotional analysis of odors of equivalent sensory intensity. *Bulletin Electro-Technical Laboratory*. 1984;**48**:796-808
- [33] Tonoike M, Seta N, Maetani T, Koizuka I, Takebayashi M. Measurements of olfactory evoked potentials and event related potentials using odorant stimuli. In: *Proceedings of the Twelfth Annual International Conference of the IEEE Engineering in Medicine and Biology Society*; Nov. 1-4, 1990. New York, NY: IEEE; 1990;**2**:912-913. DOI: 10.1109/IEMBS.1990.691487
- [34] Yamanaka T, Sobagaki H, Nayatani Y. Opponent-colors responses in the visually evoked potential in man. *Vision Research*. 1973;**13**:1319-1333
- [35] Peng W, Babiloni C, Mao Y, Hu Y. Subjective pain perception mediated by alpha rhythms. *Biological Psychology*. 2015;**109**:141-150. DOI: 10.1016/j.biopsycho.2015.05.004
- [36] Isosaka T, Matsuo T, Yamaguchi T, Funabiki K, Nakanishi S, Kobayakawa R, Kobayakawa K. Htr2a-expressing cells in the central amygdala control the hierarchy between innate and learned fear. *Cell*. 2015;**163**:1153-1164. DOI: 10.1016/j.cell.2015.10.047
- [37] Matsukawa M, Imada M, Murakami T, Aizawa S, Sato T. Rose odour can innately counteract predator odour. *Brain Research*. 2011;**1381**:117-123. DOI: 10.1016/j.brainres.2011.01.053
- [38] Murakami T, Matsukawa M, Katsuyama N, Imada M, Aizawa S, Sato T. Stress-related activities induced by predator odor may become indistinguishable by hinokitiol odor. *Neuroreport*. 2012;**23**:1071-1076. DOI: 10.1097/WNR.0b013e32835b373b

IntechOpen